Vehicle lateral control in the presence of uncertainty for lane change maneuver using adaptive sliding mode control with fuzzy boundary layer

Armin Norouzi*[,1], Reza Kazemi[1], Shahram Azadi[1]

[1]*Faculty of Mechanical Engineering, K.N. Toosi University of Technology, Tehran, Iran*

* Corresponding author: anorouzi@mail.kntu.ac.ir, +98-935-061-9855

K.N. Toosi University of Technology, Vanak Square, Molla-Sadra, Pardis, Tehran 19697, Iran

Abstract

Recent researches on advanced driver-assistance systems (ADASs) indicate great advances in terms of safety and comfort in automated driving. ADASs use control systems to perform most of the maneuvers as performed by the driver in the past. One of the useful ADASs is automatic lane change system in order to avoid accidents. This study designs the controller of an automatic lane change system for an autonomous vehicle. The control law in this study is Adaptive Sliding Mode Control (ASMC). To avoid chattering in ASMC, fuzzy boundary layer is used. Also, adaptive law is used for sliding-based switching gain. This adaptive controlling law is used to avoid the calculation of upper bound of system uncertainties. In this study, based on the boundary conditions, the vehicle lane change path planning and different maneuver periods are evaluated. To simulate the designed controller, CarSim-Simulink joint simulation model is used. This linkage leads to a full nonlinear vehicle model. The results of simulation show excellent tracking for dry road conditions and acceptable tracking in icy and wet roads in some maneuvers of above 4 seconds long.

Keywords: Autonomous vehicle, Adaptive Sliding Mode Control, Fuzzy logic system, Automatic Lane Change

1- Introduction

One of the important causes of road accidents is driver-related issues [1] including being unaware of road conditions, traffic infringement, sleeping, using drugs, etc. Advanced driver assistance systems (ADAS) are among the basic solutions to avoid driving error accidents. These systems communicate to the environment via the data received from sensors and vehicle radars and by lack of capability of the driver in steering, the car is steered automatically. National Highway Traffic Safety Administration (NHTSA) has defined different levels of car automation in 2013 [2]. According to that, level 0 vehicles are not automated. The vehicles of level 1 include driver assistance systems with limitations of lateral or longitudinal control and the rest of responsibilities are assigned to the driver. The vehicles of level 2 are relatively automatic cars with limited responsibility of some functions as simultaneous longitudinal and lateral control and the rest of responsibilities is on the account of the driver. The vehicles of level 3 include limited automatic systems. The automatic system should perform all of the tasks under some conditions and this responsibility is delegated to the driver, if necessary. According to NHTSA, the vehicles of level 4 include full automatic systems and in this level, automatic system is fully responsible for monitoring roadway and driver conditions. The lateral control of car is considered as an important part of automatic systems in levels 1 through 4, namely in overtaking and lane change maneuvers. The longitudinal control of vehicle provides the safe longitudinal distance of cars in highway and the lateral control navigates the vehicle in a desired path. The lateral control tracks the required path by creating steering angle. In this study, the vehicle lateral control is used in lane change maneuver and safe maneuver under environmental roadway conditions.

In the past 10 years, the researchers have employed different control rules including Sliding mode control (SMC) [3-12], H∞ robust control [13, 14], model predictive control (MPC) [15-20], fuzzy control [21-26], Backstepping [27, 28], adaptive control [29-31] and PID controllers [32-35] and LQR [22, 36, 37], optimization algorithms [38, 39] and solution of LMI inequalities [40] to design controllers. Sliding mode control as a non-linear control plays an important role against different friction changes of road and different velocities in the presence of parameter uncertainties [4]. Siding mode control can be combined with different control laws including fuzzy control rules [41], adaptive [6], fuzzy neural networks [8], Backstepping [28] and other control law and optimization algorithms. Li et al., [41] combination of fuzzy control rules and sliding mode and generated

the required steering of the produced maneuver. Sliding surface and its derivative after being generated by sliding mode control enters fuzzy control and the fuzzy control output generates the required command for the required maneuver. In another study done by Li et al., [8], the sliding surface acts as neural fuzzy control input and the output of this system generates car front steering. In reference [7] the sliding mode controller is modified by a PI controller. The modified controller in this study has better results compared to SMC controller. Also, using adaptive control, the switching gain of sliding mode control is updated based on sliding surface and this leads to the adaptation of control system with the environment and system conditions [6].

Başlamişli et al., [42] applied H∞ controller to improve the vehicle handling stability based on front steering system. In another study, an active steering system is designed based on H∞ controller and the relevant results at different velocities show desired path tracking [43]. Jin et al., [44] applied Gain-scheduled robust controller for lateral control of a vehicle with four electric wheels. Also, the controller design using the combination of suspension system and active steering system by Gain-scheduled robust controller led into the desired stability of vehicle.

Yoshida et al., [15] applied predictive control to control steering in lane change maneuver. In their study, the designed controller is applied on bicycle non-linear model and is simulated for different friction coefficients. Attia et al., [16] applied predictive controller on simultaneous longitudinal and lateral controller of autonomous vehicle. In another study, predictive control is applied on driver assistant system of lane change in the highways [18]. Also, Brown et al., [19] by this controller designed the autonomous vehicle tracking controller. This controller was tested for high curvature conditions and the results of study had desired path tracking. In another study done by Park [20], collision avoidance controller was designed for an autonomous vehicle based on predictive control.

Zhao et al., [21] applied fuzzy control on a vehicle model of 7 degrees of freedom (longitudinal and lateral motions of car) and evaluated the lateral control and yaw stability control using Differential Braking. The results of simulation showed that differential braking increased efficiency of lateral control systems and stability. Also, fuzzy law can combined with adaptive control law [26] and neural networks [45] and these combinations can improve the controller response.

The adaptive controllers are created based on combination with other controllers [6, 26] and for adaption and updating controller based on parameter changes. Suarez et al., [29] applied two control loops for lateral control of autonomous vehicle. Two controls are used in that study. The outer loop includes updating feedforward gain and in the inner loop, Model Following Controller (MFC) is used to create the system stability. Khosravi et al., [31] applied predictor-based model reference adaptive control and LQR controller for lateral control of vehicle in the presence of uncertainties.

Emirler et al., [32] designed PID controller based on parameter space approach of autonomous vehicle controlled the lateral and angular errors of yawn. The use of PI control with feedback & feedforward controllers [34] or pole placement [35] presented good results for desired tracking. Also, by fuzzification [33] or adaption [46], of PID controller coefficients, we can improve the non-linear behavior of this controller to have good response to the parameters changes and have desired tracking. Anderson et al., [36] integrated the signal of driver response with the signal of LQR controller based on desired roadway and created final steering system of the vehicle. Moreover, Actuator Fault detectors have been used in another research for a vehicle with active front steering [47].

Feng et al., [38] applied fuzzy-neural networks (FNN) controller with genetic algorithm for lateral control of vehicle to perform lane change maneuver. In another study, the vehicle tracking control is designed using PSO optimization algorithm based on PID, LQR controllers [39]. Enache et al., [40] applied LMI (linear matrix inequality) and BMI (bilinear matrix inequality) optimization methods to design the controller of lane keeping system. The various control methods performed by researchers are mentioned. In addition, different heuristic methods are applied as the result of innovative integration of these methods. In the majority of researches, software simulation is used to test the designed controller based on dynamic models (normally by bicycle two degree model). Among them, CarSim-Simulink joint simulation is used as one of the best software in this regard [7, 20, 35, 44, 48-53]. This simulation system presents full vehicle model consisting of all degrees of freedom and different vehicle sub-systems. By linking this software and applying the designed controller in Simulink space, we can perform different simulations by the software.

As noted in the literature review, many of existing researches have not presented a controller that fully controls the vehicle in different conditions of the road. The aim of this study is at addressing various issues of existing works. The goal of this study is to present a control which is capable of controlling the lane change maneuvers at any time and in different environmental conditions. Considering the existing uncertainties in the system, particularly the friction between the road and the tires, the sliding mode controller has been opted. In addition, to avoid the prior knowledge of ranges of uncertainties, adapting rules have been added to the sliding mode controller. It is clear that one of the main issues with

this controller is the chattering. Adding a boundary layer will terminate this issue, however it also increases the tracking error. Therefore, the boundary layer has been designed using fuzzy logics rules in a way that is near the sliding surface at any given time during the maneuver. As a result, while the tracking error will be reduced, the chattering will be avoided.

In this study, by adaptive sliding mode control (ASMC) with fuzzy boundary layer, a lateral control system is designed for automatic lane change system. This paper consists of four sections. The first section explores the lane change path planning based on the boundary conditions of vehicle and environment and a path with Quintic function. The second section presents a dynamic model and the dynamic model is achieved in terms of position and orientation errors. This study applies two degrees of freedom bicycle model in controller design. The third section presents a control strategy and designs an adaptive sliding mode controller for automatic lane change system. It also defines Lyapunov function and uses Lyapunov stability to support the adaptive robust controller stability. Fourth section elaborates on the simulation of lane change maneuvers and evaluates different conditions of environment and vehicle. The simulation in this study is performed using CarSim software linked with Matlab/Simulink. The results of simulation show that by the increase of period of lane change maneuver, the numerical value of friction, based on the road condition and reduction of car velocity, presents better results and for critical conditions, the lateral stability is preserved.

2- Lane change path planning

Various researches have been conducted on the design of lane change maneuver and one of the common methods for path planning is using mathematical functions such as Quintic function [54]. Equation (1) is considered as candidate function to design lane change path. At the beginning and the end of the maneuver, the vehicle moves in a straight lane and the acceleration and lateral velocity are zero. The lateral position at maneuver starting time is zero (Equation 2) and for the end of maneuver is equal to the distance of the center lanes of origin and destination (Equation 3). t_1 is the starting time of maneuver and T is the ending time of maneuver. Figure 1 shows the lane change based on Quintic function in which the boundary conditions are also shown.

$$y(t) = at^5 + bt^4 + ct^3 + dt^2 + et + f \tag{1}$$

$$\begin{aligned} \dot{y}|_{t=t_1} &= 0 \\ \ddot{y}|_{t=t_1} &= 0 \\ \dot{y}|_{t=T} &= 0 \\ \ddot{y}|_{t=T} &= 0 \end{aligned} \tag{2}$$

$$\begin{aligned} y|_{t=t_1} &= 0 \\ y_1|_{t=T} &= -3.75 \end{aligned} \tag{3}$$

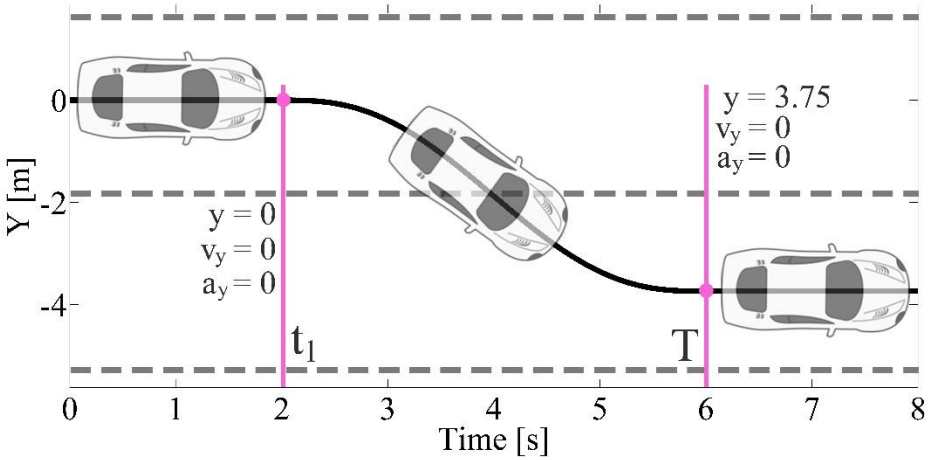

Figure 1 The lane change path based on Quintic function

By applying boundary conditions (2), (3) to candidate function of Equation (1), the following Equation is achieved:

$$\begin{bmatrix} t_1^5 & t_1^4 & t_1^3 & t_1^2 & t_1 & 1 \\ 5t_1^4 & 4t_1^3 & 3t_1^2 & 2t_1 & 1 & 0 \\ 20t_1^3 & 12t_1^2 & 6t_1 & 2 & 0 & 0 \\ T^5 & T^4 & T^3 & T^2 & T & 1 \\ 5T^4 & 4T^3 & 3T^2 & 2T & 1 & 0 \\ 20T^3 & 12T^2 & 6T & 2 & 0 & 0 \end{bmatrix} \begin{bmatrix} a \\ b \\ c \\ d \\ e \\ f \end{bmatrix} = \begin{bmatrix} 0 \\ 0 \\ 0 \\ -3.75 \\ 0 \\ 0 \end{bmatrix} \quad (4)$$

By solving the above matrix equation, path coefficients are designed in terms of the starting (t_1) and end time (T) of maneuver path. By entering this path to control system and calculation of desired yaw (ψ_d), the autonomous vehicle is controlled in the desired maneuver path.

3- Modelling

In this study, the vehicle dynamic model of 2 DOF, called bicycle, is used. Figure 2 depicts the vehicle bicycle model. The bicycle model in this study has two degrees of freedom including yaw rate and lateral sliding angle of the vehicle.

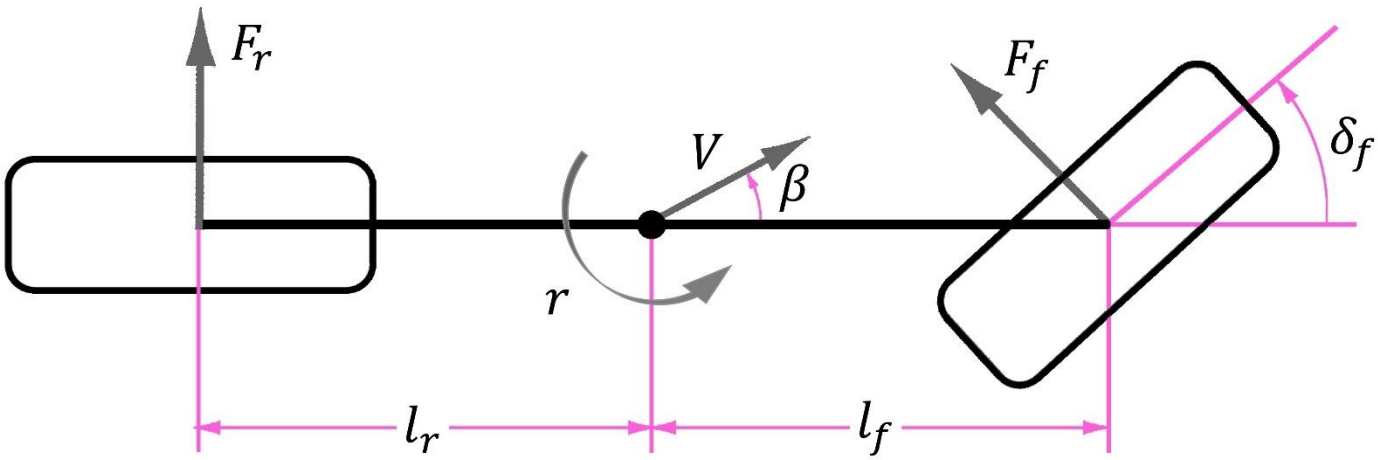

Figure 2 The two degrees of freedom model of bicycle

The dynamic equations of this model are shown in Equation (5) [55].

$$\dot{\beta} = \left(-2\frac{c_f^* + c_r^*}{mV_x}\right)\beta + \left(-1 + 2\frac{l_r c_r^* - l_f c_f^*}{mV_x{}^2}\right)r + (2\frac{c_f^*}{mV_x})\delta_f$$
$$\dot{r} = (2\frac{l_r c_r^* - l_f c_f^*}{J})\beta + (-2\frac{c_f^* l_f^2 + c_r^* l_r^2}{JV_x})r + (2\frac{l_f c_f^*}{J})\delta_f \quad (5)$$

This dynamical model, neglecting roll, bounce and pitch, has been used to design the controller along with the following assumptions: [55]

Assumption 1: Lateral sliding angle, steering angles, and lateral sliding angles of front and rear tires are assumed to be neglected.

Assumption 2: The longitudinal velocity of vehicle is constant and its value has been assumed to be between v1 and v2.

Assumption 3: The relationship between lateral forces of tire and sliding angle is assumed to be linear.

In this model, lateral forces of tire are equal to Equation (6) [56].

$$F_f = \alpha_f c_f^* = \alpha_f c_f \mu$$
$$F_f = \alpha_r c_r^* = \alpha_r c_r \mu \quad (6)$$

Where, α is sliding angle, c^* nominal lateral stiffness of tires, c_f and c_r are, respectively, the cornering stiffness of front and rear tires and μ is the friction coefficient. The vehicle model has some uncertainties and by robust control, we attempt to make the system robust against these uncertainties. In this study, the parameters are considered as uncertainties of the longitudinal velocity of vehicle and friction coefficient. Since longitudinal velocity is controlled by the driver's command or longitudinal controller, and has various values, this parameter is considered as uncertainty parameter such that the proposed controller system can preserve its robustness against variations. Table 1 shows the vehicle parameters.

Table 1- The vehicle parameters in this study [57]

Symbol	Variable name	Value	Unit
μ	Road friction coefficient	[μ_1-μ_2]	-
m	Mass	1704.7	[kg]
J	Yaw moment of inertia	3048.1	[kg.m^2]
l_f	Front axle-COG distance	1.035	[m]
l_r	Rear axle-COG distance	1.655	[m]
C_f	Cornering stiffness of front tire	105850	[N/rad]
C_r	Cornering stiffness of rear tire	79030	[N/rad]
v	longitude velocity	[v_1-v_2]	[m/s]

In this study, the changes of friction interval are ranging from 0.1 to 1. The minimum and maximum velocity is 5 m/s and 40 m/s, respectively. For controller simulation, 30, 40 m/s and dry, wet and frozen roads were used. The coefficient of adhesion for different road conditions is shown in Table 2.

Table 2- Coefficient of adhesion for different climatic conditions [56]

Pavement type	Coefficient of adhesion
Dry	1
Wet	0.5
Ice	0.15

For controller design, position and orientation error with respect to the road errors are defined as follows:

$\boldsymbol{e_1}$ the distance of the C.G. of the vehicle from the center line of the lane

$\boldsymbol{e_2}$ the orientation error of the vehicle with respect to the road

These errors are shown schematically in Figure (3). These errors are defined using the system states as follows [55]:

$$\dot{e}_1 = \dot{y} + V_x(\psi - \psi_d) = V_x(\beta + \psi - \psi_d)$$
$$e_2 = \psi - \psi_d \quad (7)$$

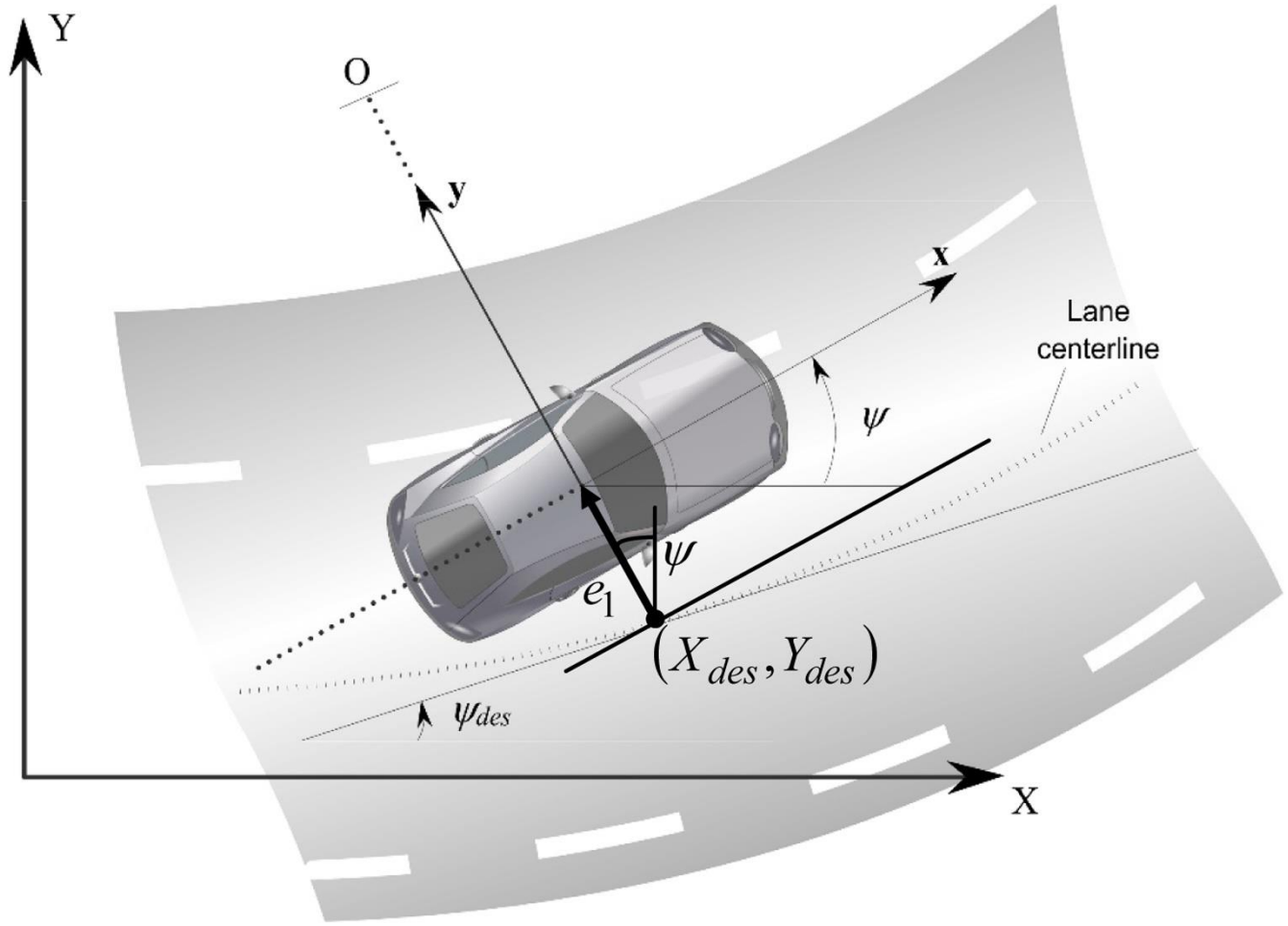

Figure 3 Lateral error and coordinate of vehicle in body fixed and global coordinate [55]

Using Equations (5-7), the dynamic equation is achieved in term of position and orientation errors as:

$$\begin{aligned} \ddot{e}_1 &= a_{11}\dot{e}_1 + a_{12}e_2 + a_{13}\dot{e}_2 + b_1\delta_f + d_1\dot{\psi}_d \\ \ddot{e}_2 &= a_{21}\dot{e}_1 + a_{22}e_2 + a_{23}\dot{e}_2 + b_2\delta_f + d_2\dot{\psi}_d - \ddot{\psi}_d \end{aligned} \tag{8}$$

The coefficients of this equation are shown in Appendix 1. Also, the upper and lower bound values of Equation (8) are based on the mentioned uncertainties in Appendix 2. Based on the equations in reference [55] and Figure 3, the desired yaw angle of road is defined as in Equation (9). Also, the final output in global coordinates is achieved as Equation (10).

$$\psi_d = tan^{-1}\frac{\dot{Y}_{des}}{\dot{X}_{des}} \approx \frac{\dot{Y}_{des}(t)}{V_x} \tag{9}$$

$$\begin{aligned} X &= \int_0^t V_x\, cos(\psi_d)\, dt - e_1 sin\,(\psi) \\ Y &= \int_0^t V_x\, sin(\psi_d)\, dt + e_1\, cos(\psi) \end{aligned} \tag{10}$$

4- Controller design

The sliding mode controller system is considered as an appropriate controller in coping up with uncertainties. In this study, the adaptive sliding model with fuzzy boundary layer is used. By creating boundary layer to avoid chattering of sliding mode controller, an intentional error is introduced to system. As the fuzzy boundary layer is closer to sliding

surface, it creates less error compared to that of fixed boundary layer and chattering is also avoided. Adaptive control law shows switching gain based on the variations of sliding surface.

In this section, just firstly we define sliding surface based on errors and then we design a controller. In the next section, the fuzzy boundary layer and adaptive control law are applied and finally by definition of Lyapunov function, the controller stability is proved as analytic. As the vehicle model has two degrees of freedom, the sliding surface is selected as Equation (11):

$$s = \left(\frac{d}{dt} + \lambda\right)\tilde{x} = \dot{e}_1 + d\dot{e}_2 + \lambda(e_1 + de_2) \tag{11}$$

Where, λ is strictly positive constant [58] and $\tilde{x}$ is tracking error:

$$\tilde{x} = e_1 + de_2 \tag{12}$$

Where, d is the distance of sensor from the head of vehicle to the mass center of the car. $\tilde{x}$ is shown schematically in Figure 4.

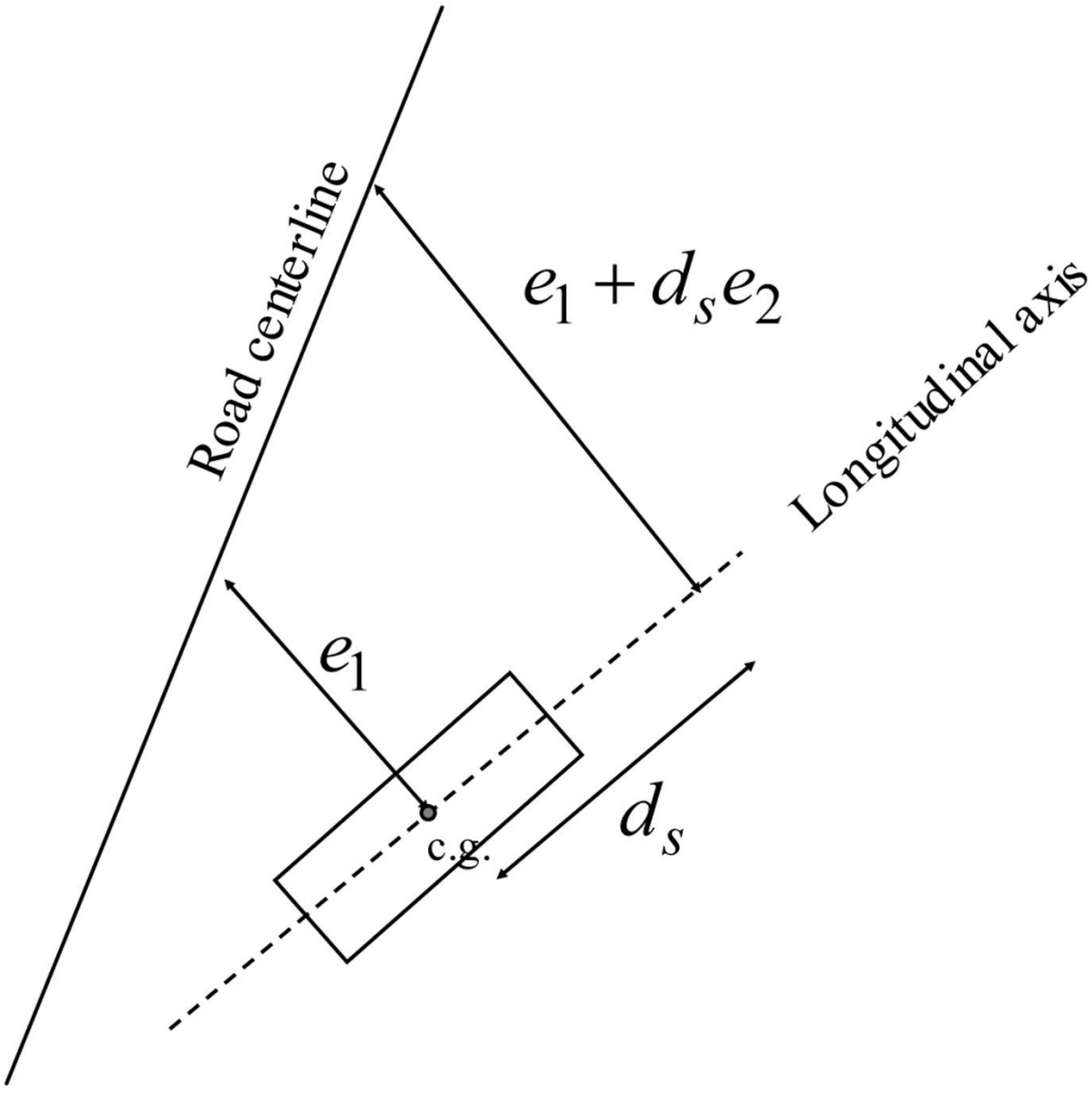

Figure 4 The measurement of Look ahead lateral to the center line of the road [55]

The above sliding surface has some advantages such as:

- A problem of order n is converted to a problem of order one.
- This is a filter of order *n* which leads the chattering to be highly reduced.
- The above surface has the fastest response among linear systems without vibrations. However, many others have used different poles.

Although in Figure 4, these errors are presented for lane keeping system but by applying the desired path, we can use this error for path tracking error.
Differentiating the sliding surface, we have:

$$\dot{s} = A_4\dot{e}_1 + A_2e_2 + A_5\dot{e}_2 + bu + D\dot{\psi}_d - d\ddot{\psi}_d \quad (13)$$

Where u is the angle of front steering of the vehicle:

$$u = \delta_f \quad (14)$$

According to Reference [58], the best control law for $\tilde{x}$ error is achieved by $\dot{s} = 0$. Thus, by putting the derivate of sliding surface (Equation 13) equal to zero, the best control law is achieved:

$$u_{eq} = -\hat{b}^{-1}(\hat{u}) \quad (15)$$

Where û is defined as:

$$\hat{u} = \hat{A}_4\dot{e}_1 + \hat{A}_2e_2 + \hat{A}_5\dot{e}_2 + \hat{D}\dot{\psi}_d - d\ddot{\psi}_d \quad (16)$$

According to Reference [58], sliding condition is defined as follows:

$$\frac{1}{2}\frac{d}{dt}s^2(t) \le \eta|s(t)| \quad (17)$$

Where η is a strictly positive constant [58]. To satisfy this condition, a term is added to u_{eq}:

$$u = u_{eq} - k\hat{b}^{-1}sign(s) \quad (18)$$

To establish sliding condition (Equation 18), the range of k is yielded similar to reference studies [58]:

$$k \ge \gamma(F + \eta) + (\gamma - 1)|\hat{u}| \quad (19)$$

Equations F, $\hat{A}$, $\hat{b}$, $\hat{D}$ and γ are shown in Appendix (2).
To avoid chattering, instead of sign function, we can use saturate function. Saturate function is shown in Equation (20)

$$sat\left(\frac{s}{\phi}\right) = \begin{cases} 1 & \frac{s}{\phi} > 1 \\ \frac{s}{\phi} & -1 < \frac{s}{\phi} < 1 \\ -1 & \frac{s}{\phi} < -1 \end{cases} \quad (20)$$

Where ϕ is the thickness of the boundary layer. Thus, the final equation of SMC controller is achieved as:

$$u = u_{eq} - k\hat{b}^{-1}sat(\frac{s}{\phi}) \quad (21)$$

In this study, ϕ is entered based on fuzzy logic[59, 60] and sliding surface in Equation (21). The input of this fuzzy rule is sliding surface and its output is ϕ value and it is changed by changing the sliding surface. Generally, the fuzzy system rule is as by increasing the value of s, the boundary layer ϕ is increased and by reduction of the values, this value is reduced. By this logic, fuzzy rules are as:

R1: If *s* is **Z** then ϕ is **Z**
R2: If *s* is **PS1** and **NS1** then ϕ is **S1**
R3: If *s* is **PS2** and **NS2** then ϕ is **S2**
R4: If *s* is **PM1** and **NM1** then ϕ is **M1**
R5: If *s* is **PM2** and **NM2** then ϕ is **M2**
R6: If *s* is **PB1** and **NB1** then ϕ is **B1**
R7: If *s* is **PB2** and **NB2** then ϕ is **B2**
R8: If *s* is **PB3** and **NB3** then ϕ is **B3**

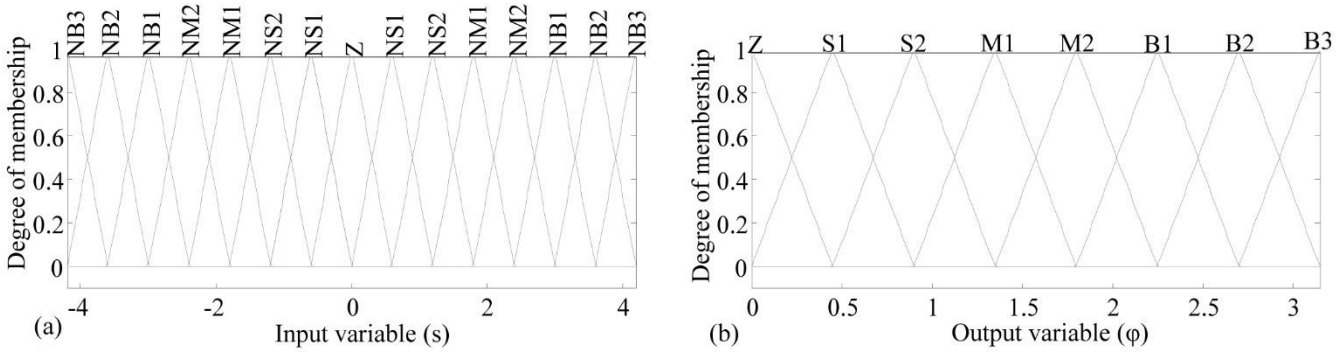

Figure 5 a) the input of fuzzy rules is the slidng surface b) The output of fuzzy rules is the boundary layer.

This specific number of fuzzy rules has been chosen to give a generalization sense to the controller, so that it expands at shorter distances from the boundary layer at any time. It is obvious that in very low frictions and through eliminating steep maneuvers, the system is controllable using fewer rules.

The next section includes applying adaptive control law on sliding mode controller of the previous section. The adaptive control law is defined as Equation (22) in which $\hat{\beta}$ is switching gain and presents an estimation of k [61]:

$$\dot{\hat{\beta}}(t) = \Gamma|s(t)| \qquad \hat{\beta}(0) = 0 \tag{22}$$

Thus, control command is achieved based on adaptive sliding model controller:

$$u_{ASMC} = u_{eq} - \hat{\beta}\Gamma\hat{b}^{-1}sat(\frac{s}{\phi}) \tag{23}$$

Where, Γ is constant and positive. This constant value enables use to select the adpative velocity for sliding gain (switching gain). To select it, there are some constraints as evaluated in the stability section. It is worth to mention that $\hat{\beta}$ has no association with the lateral sliding angle of the vehicle.

To evlauate the stability of the designed controller, the candidate Lyapunov function is selected as:

$$V(t) = \frac{1}{2}s^2 + \frac{b\hat{b}^{-1}}{2}\tilde{\beta}^2 \tag{24}$$

Where, $\tilde{\beta}$ is defined as:

$$\tilde{\beta} = \hat{\beta} - k \tag{25}$$

k is achieved using Equation (19). To eavluate the Lyapunov function, the Lyapunov candidate function is derived:

$$\dot{V}(t) = s\dot{s} + b\hat{b}^{-1}\tilde{\beta}\dot{\tilde{\beta}}$$

$$\dot{V}(t) = s[A_4\dot{e}_1 + A_2e_2 + A_5\dot{e}_2 + D\dot{\psi}_d - d\ddot{\psi}_d + b\left\{-\hat{b}^{-1}(\hat{u}) - \hat{\beta}\Gamma\hat{b}^{-1}sat\left(\frac{S}{\varphi}\right)\right\}] + b\hat{b}^{-1}(\hat{\beta} - k)\Gamma|s(t)|$$

$$\dot{V}(t) = s[A_4\dot{e}_1 + A_2e_2 + A_5\dot{e}_2 + D\dot{\psi}_d - d\ddot{\psi}_d + b\left\{-\hat{b}^{-1}\left(\hat{A}_4\dot{e}_1 + \hat{A}_2e_2 + \hat{A}_5\dot{e}_2 + \hat{D}\dot{\psi}_d - d\ddot{\psi}_d\right) - \hat{\beta}\Gamma\hat{b}^{-1}sat\left(\frac{S}{\varphi}\right)\right\}] + b\hat{b}^{-1}(\hat{\beta} - k)\Gamma|s(t)|$$

$$\dot{V}(t) \le \left|\bar{A}_4\dot{e}_1 + \bar{A}_2e_2 + \bar{A}_5\dot{e}_2 + \bar{D}\dot{\psi}_d\right||s(t)| + \left|1 - b\hat{b}^{-1}\right||\hat{u}||s(t)| - b\hat{b}^{-1}\hat{\beta}\Gamma|s(t)| + b\hat{b}^{-1}\hat{\beta}\Gamma|s(t)| - b\hat{b}^{-1}\hat{\beta}\Gamma|s(t)|$$

According to Appendix 3, we have :

$$\dot{V}(t) \le F|s(t)| + |1-\gamma^{-1}||\hat{u}||s(t)| - \gamma^{-1}(\gamma(F+\eta) + (\gamma-1)|\hat{u}|)\Gamma|s(t)|$$

$$\dot{V}(t) \le (1-\Gamma)(F + |1-\gamma^{-1}||\hat{u}|)|s(t)|) - \eta\Gamma|s(t)|$$

Since η is strictly positive constant, the derivative of Lyapunov function becomes negative, only if Γ is bigger than 1, thus we have:

$$\Gamma \ge 1 \qquad \rightarrow \qquad \dot{V}(t) \le 0 \tag{26}$$

Hence, by selecting of Γ bigger or equal to 1, we can guaranty the system stability based on Lyapunov stability. Figure 6 shows the block diagram of adaptive sliding model control with fuzzy boundary layer.

There are two ways to measure slip angle of a tire: on a vehicle when it is moving, or using a dedicated device. When the vehicle is moving, optical methods can be used to measure slip angle. In addition, GPS devices and inertial methods (or both) can be utilized. On the other hand, various testing devices have been developed to measure slip angle of a tire in a controller environment. They often use the inner or outer surface of rotating drums, sliding planks, conveyor belts.

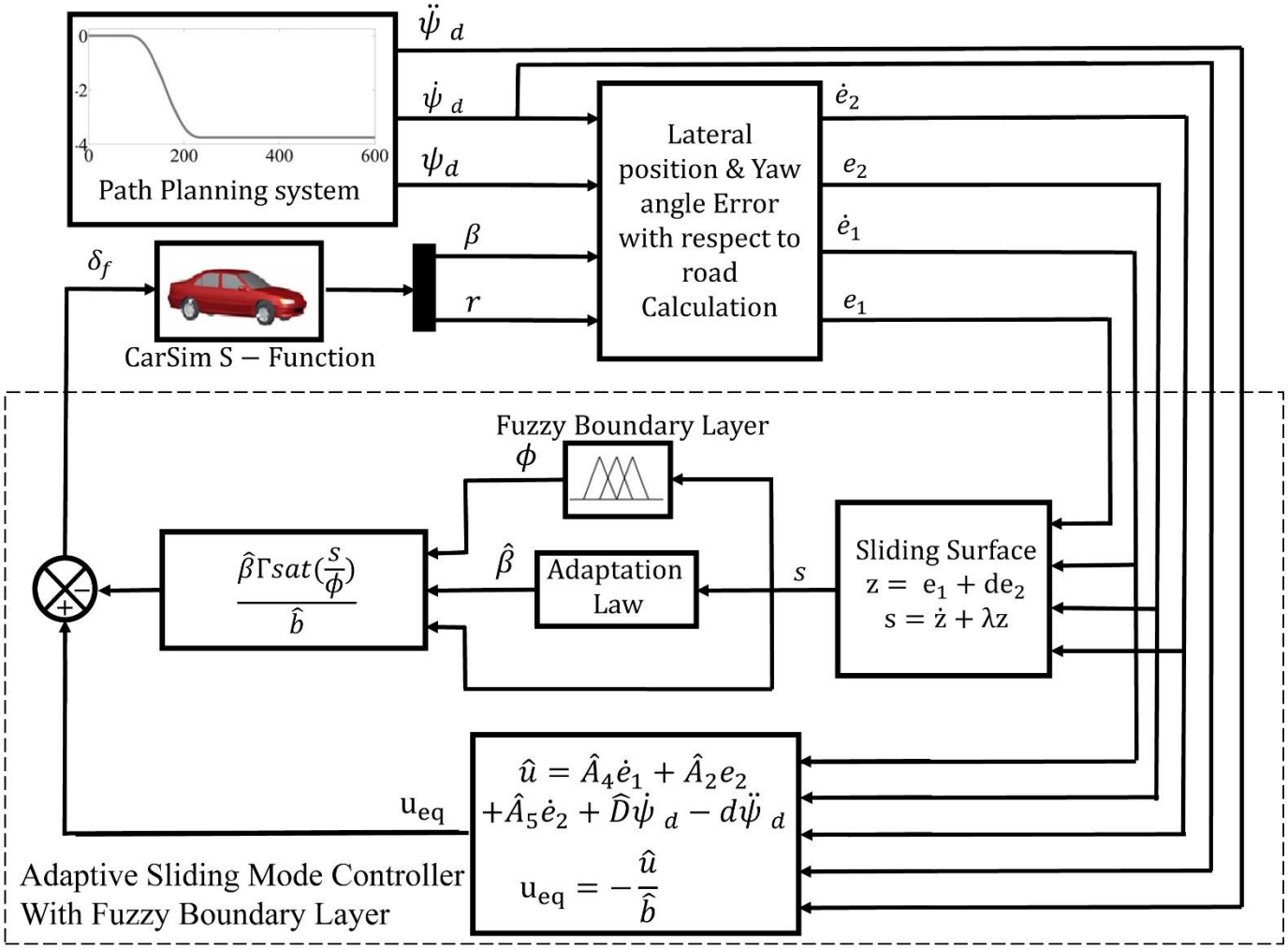

Figure 6 The block diagram of adaptive sliding model control with fuzzy boundary layer for automatic lane change system

4- Discussion and Results

In this section, the designed path for lane change maneuver is inputted into the controller, based on the equations in the modeling section. Simulation is performed using CarSim linked with Simulink Software and F-Class model is chosen as shown in Table 1. By linking CarSim to Simulink the full vehicle model with high DOF and system's non-linearities is obtaind. The simulation of the proposed controller has been conducted using this full vehicle model.

In addition to mentioned advantages such as the lack of requirement to know the ranges of uncertainties due to the use of adaptive rules, and reduced tracking error resulting from adding fuzzy boundary layer, the performance of this controller has been compared against that of sliding mode controller. Figures 7 and 8 compare the performance of the two controllers in dry (friction = 1) and wet (friction = 0.15) roads. The length of maneuvers have been considered as 3 and 5 seconds to demonstrate the performance of each controller.

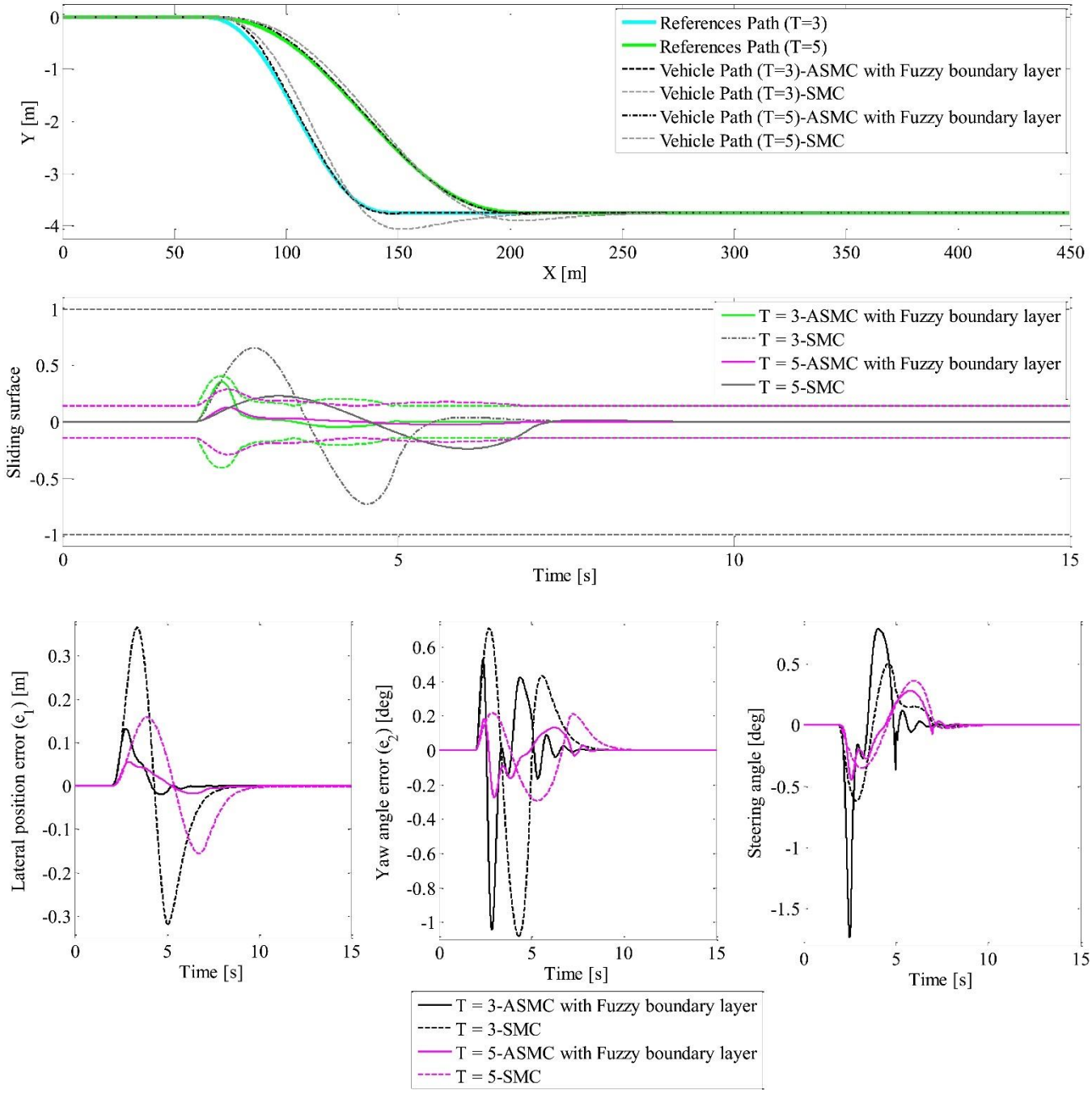

Figure 7 Comparison of the two controllers for maneuvers of 3 and 5 seconds long and dry road (μ= 1)

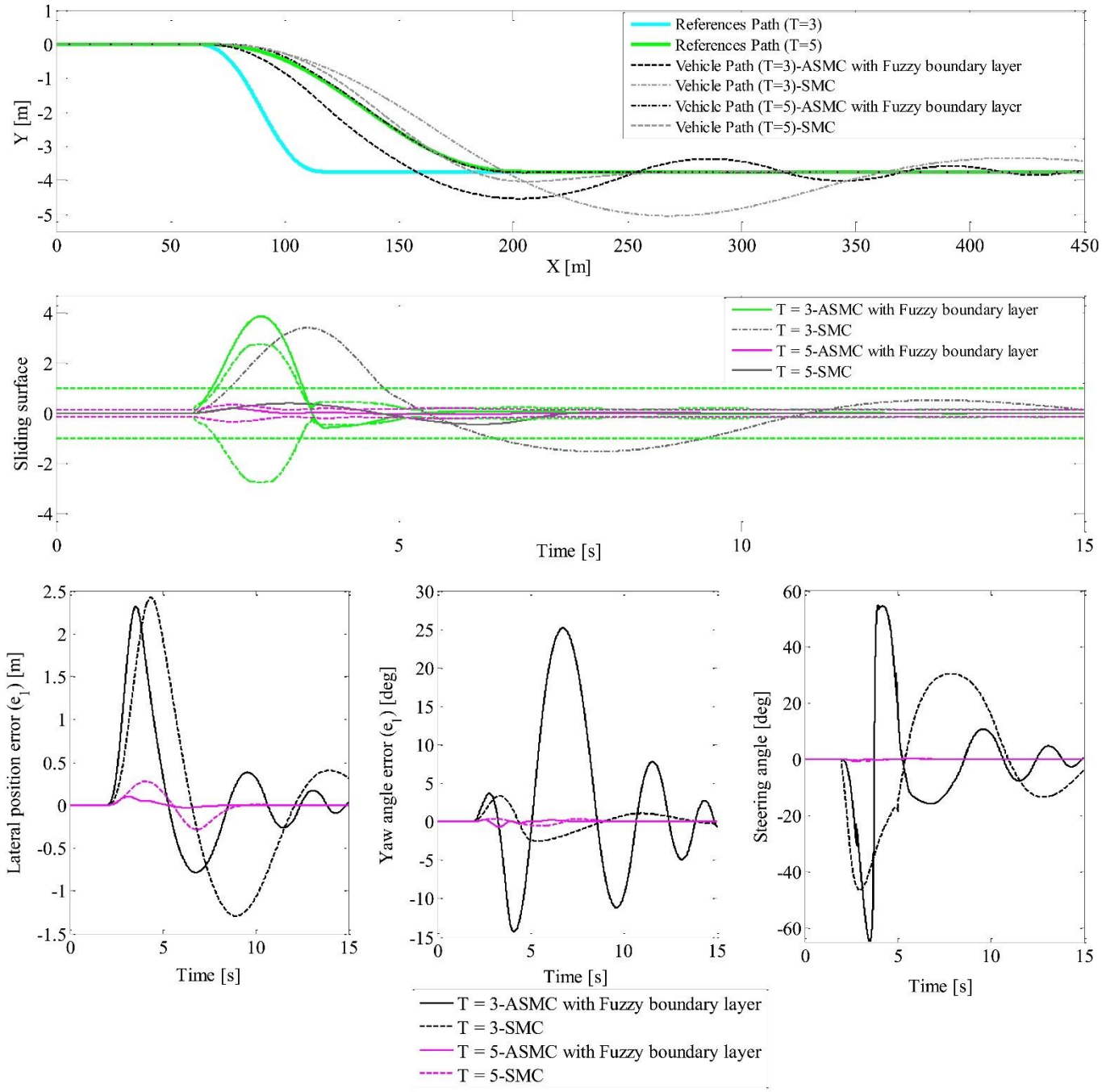

Figure 8 Comparison of the two controllers for maneuvers of 3 and 5 seconds long and icy road (μ= 0.15)

As shown in figures above, the performance of the proposed controller is much better than that of sliding mode controller for both dry and wet roads. In the maneuver of 3 seconds long, due to the very low friction in the case of icy road and the high velocity, both controllers have fluctuations in path tracking, however, the fluctuations of the proposed controller have been dumped and finally the full tracking is achieved. The reason of high fluctuations is the low friction of the road. In fact, even a human driver is not able to control the vehicle. Some suggestions have been provided at the end of this section to improve this performance.

In this paper, for the purpose of simulation, lane change paths with T values from 2s to 6s at longitudinal velocities from 30m/s to 40m/s are used. The controller is simulated for three states of dry road (friction 1), wet road (friction 0.5) and frozen road (friction 0.15). Figures 9-11 depict the simulation of autonomous car at a velocity of 30 m/s and different frictions, and Figures 12-14 illustrate the simulation for a longitudinal velocity of 40m/s. In these figures, inset (a) includes reference *x,y* and the vehicle for different *T* (lane change duration) values. Inset (b) shows the sliding surface against time for different *T* values. The dashed curve illustrates the fuzzy boundary layers. Insets (c) and (d) show lateral e_1 and angular e_2 errors against different T values. Insets (e) to (h) show steering angle (control output), yaw rate, lateral sliding angle and roll angle against different T values.

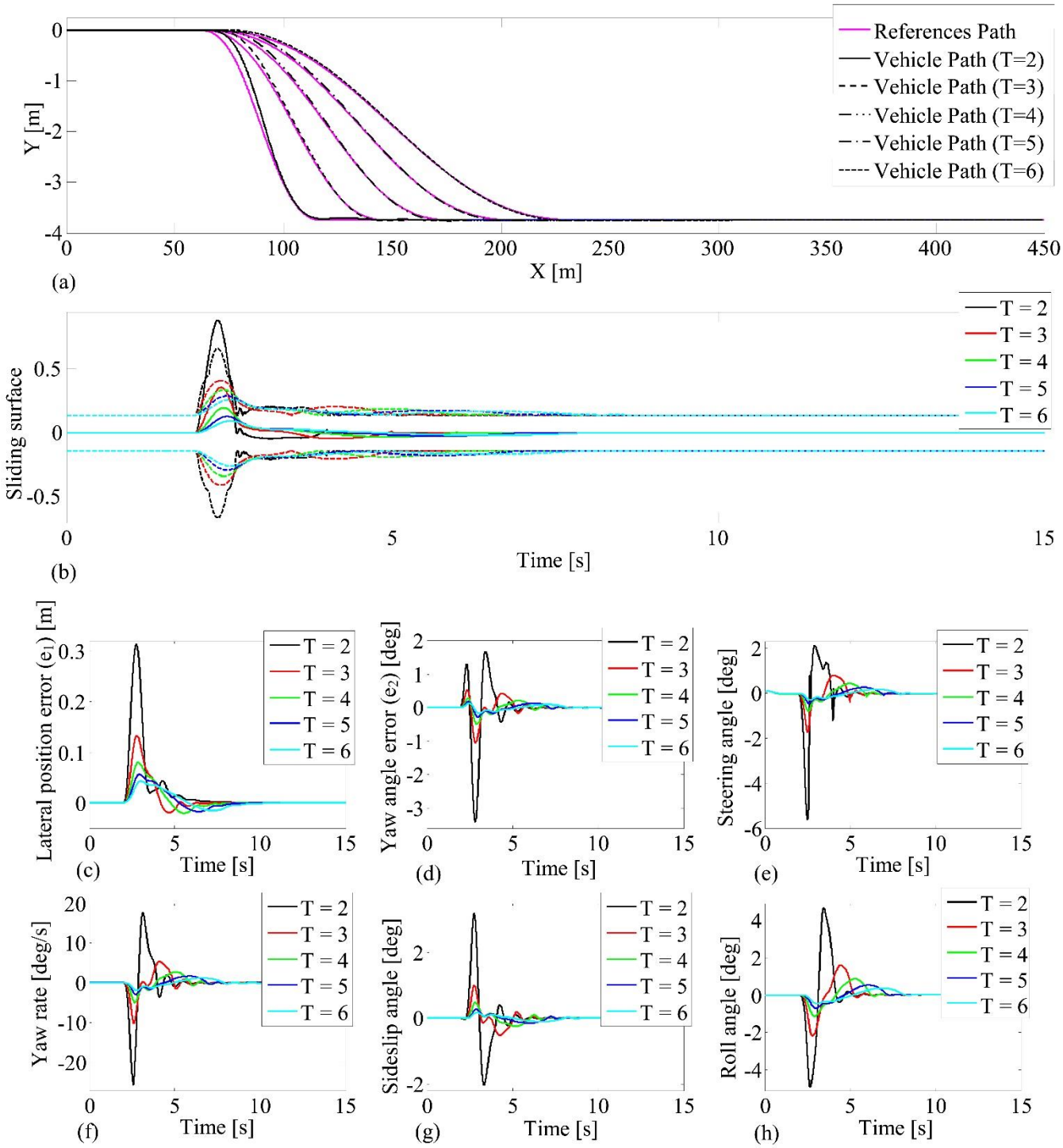

Figure 9 The simulation of longitudinal velocity 30m/s and dry road (μ= 1)

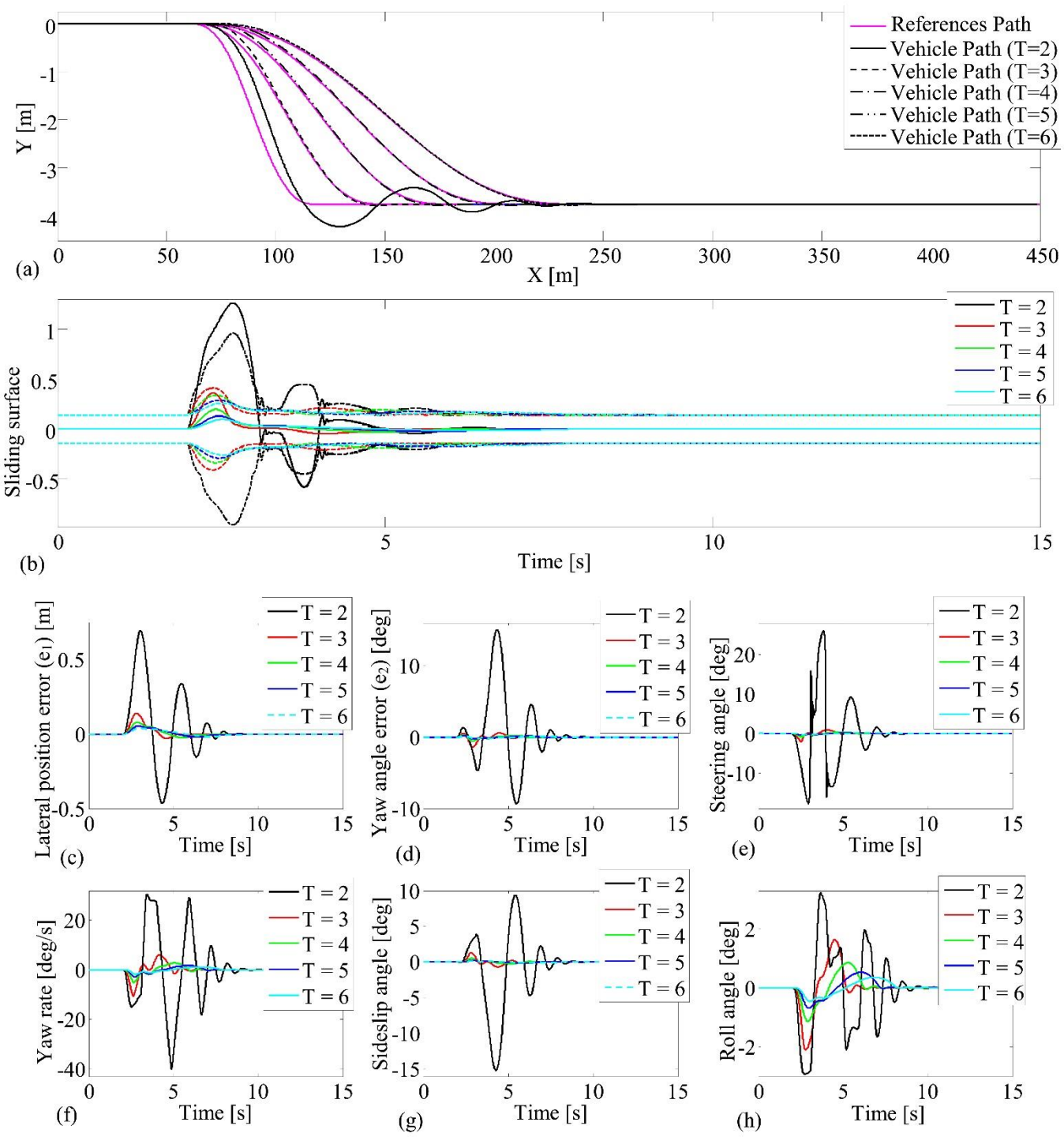

Figure 10 The simulation of longitudinal velocity 30m/s and wet road (μ= 0.5)

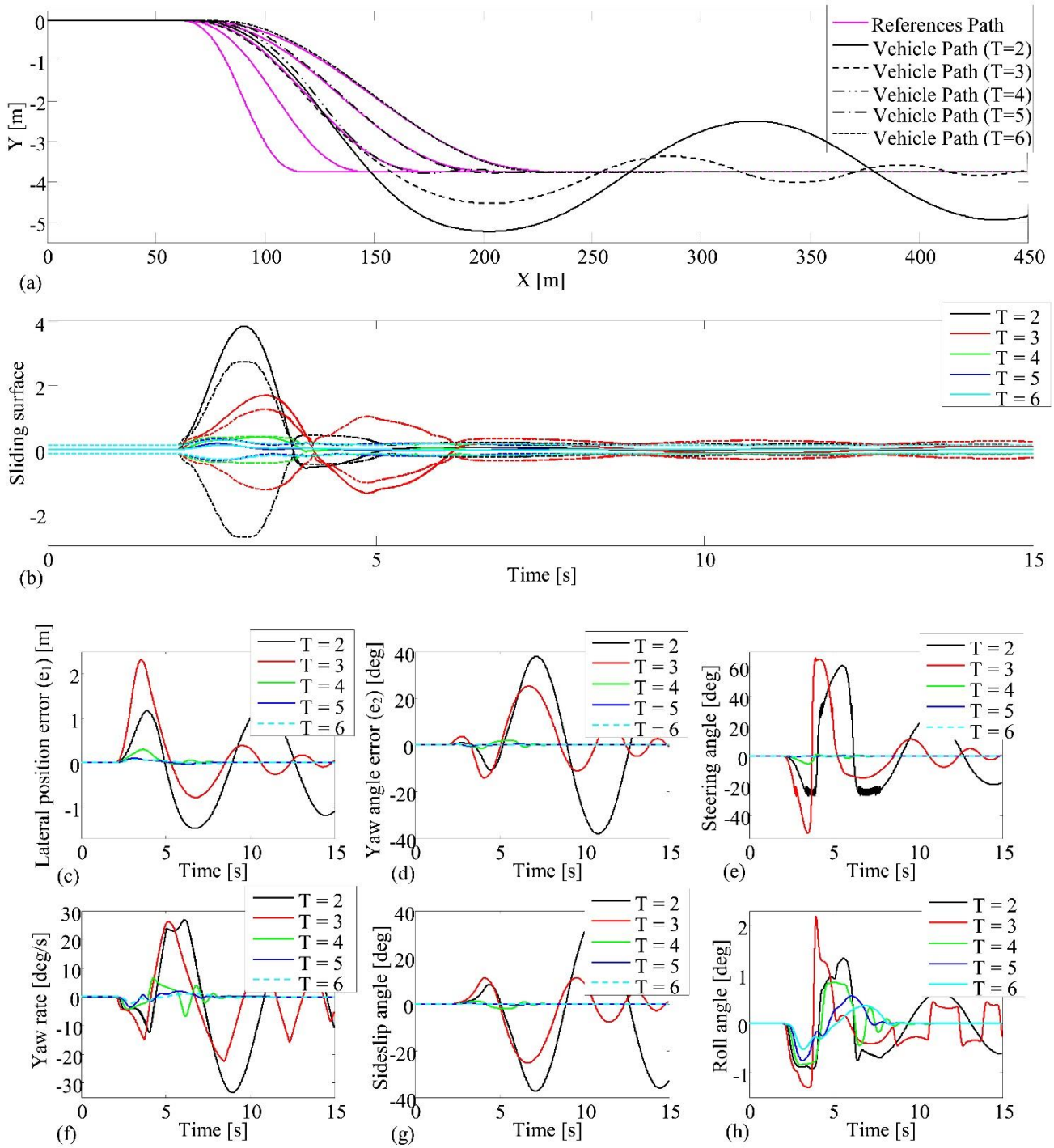

Figure 11 The simulation of longitudinal velocity 30m/s and icy road (μ= 0.15)

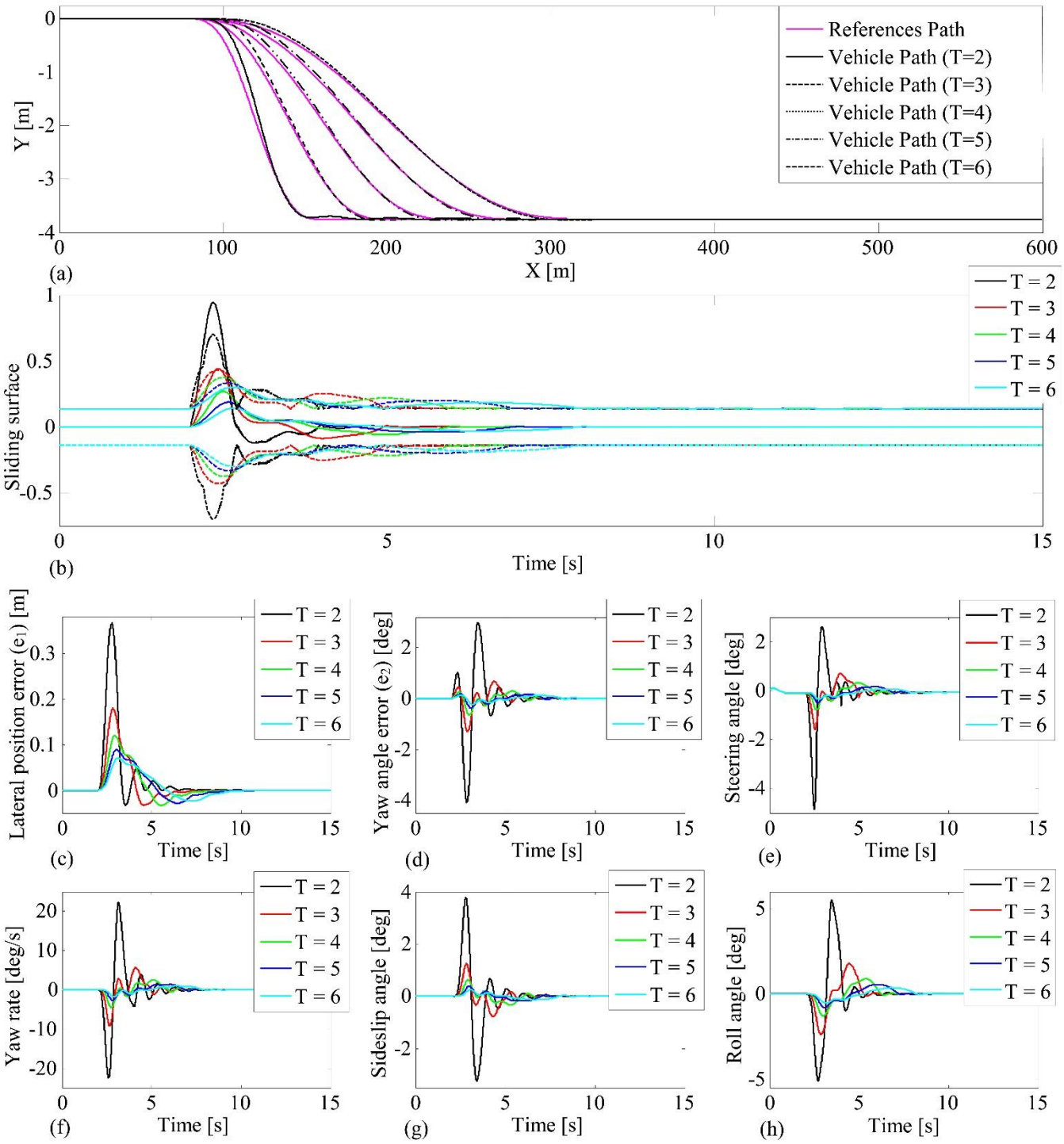

Figure 12 The simulation of longitudinal velocity 40m/s and dry road (μ= 1)

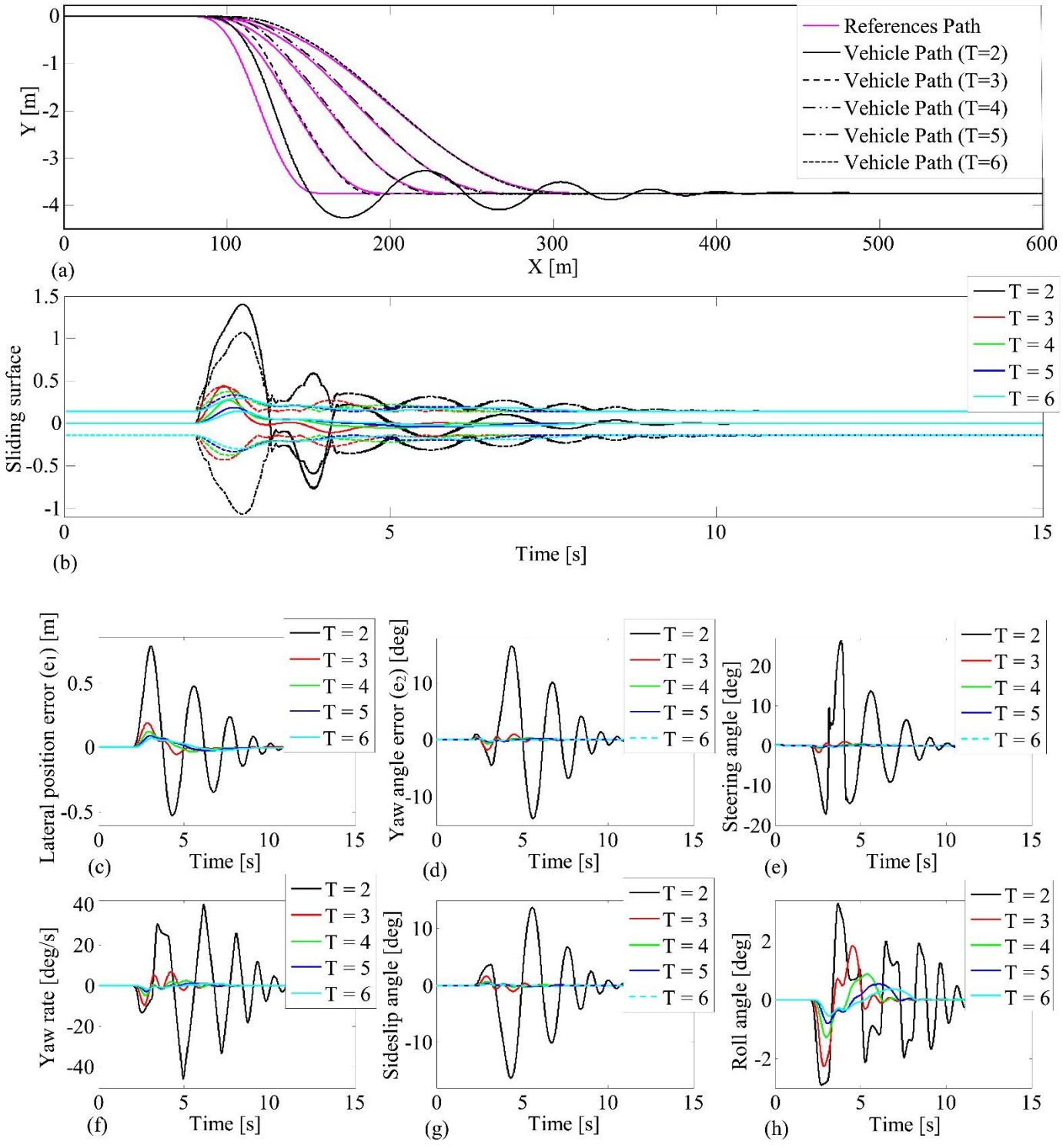

Figure 13 The simulation of longitudinal velocity 40m/s and wet road (μ= 0.5)

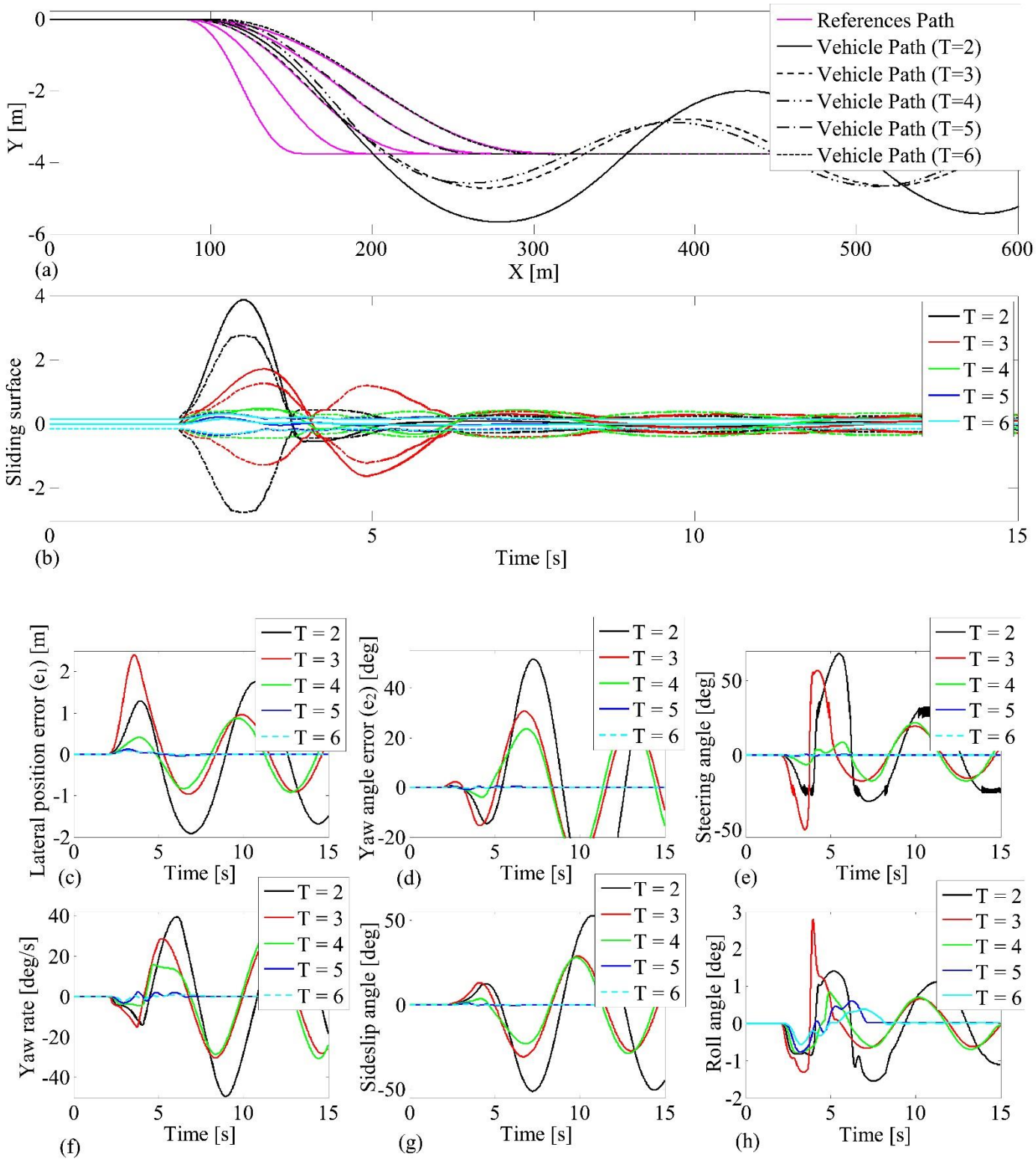

Figure 14 The simulation of longitudinal velocity 40m/s and icy road (μ= 0.15)

As shown in Figures 9 and 12, the system presents a perfect performance. The path tracking is completely performed (except when *T* is equal to 2s). Even at *T*=2s, path tracking shows high performance. The sliding surface is fully surrounded by the boundary layer. When *T* is equal to 2s, only in the vicinity of maximum, the sliding surface has been located outside the boundary layer, however, no chattering can be seen in the system. From an engineering perspective,

it is shown that for short maneuvers in terms of time, steering angle, yaw rate, lateral sliding angle and roll angle are maximum and by the increase of maneuver time, the angles are reduced and the full path tracking is possible. The simulation, for friction of 0.5 (wet road), is shown in Figures 10 and 13 when *T* is equal to 2s. Although there appears high fluctuations, but after a short period, the system achieves the stability state. The effect of these fluctuations can be seen as lateral and angular error, high yaw rate, high steering angles, high roll and high lateral sliding. For maneuvers with other periods, a desired tracking of reference path is performed. In the frozen road, as shown in Figures 11 and 14, the behaviors for two velocities are similar, however there exists the difference that the maximum values are higher for higher velocities. In this case, for *T*=2s, the controller attempts to keep the system on the destination lane in a sinusoidal motion and as shown in sliding surface, this surface has no fluctuations. For *T*=3s, the car has high fluctuations but finally these fluctuations are damped and the car moves on the lane and after a short period, tracking with high accuracy is achieved. For maneuvers of about 4s at a velocity of 30m/s, and for maneuvers of about 5s at a velocity of 40m/s, the vehicle follows the designed path and we observe the full path tracking. For high frictions, we observe remarkable steering angles for maneuver periods of 2 or 3 seconds long. These angles cannot be practically applied by the front wheel. For these maneuvers, the lateral sliding angle and yaw rate have also high values, but roll angle is low due to sliding. When the friction is high, despite the severe maneuver, the lateral force of wheels resist against the friction of surface, and instead of sliding in the target lane, it starts rolling. Therefore, roll angle is higher for high frictions.
For better comparison of controller performance for different velocities and frictions, Root mean square (RMS) of lateral and angular errors is achieved for different maneuver times, velocities and frictions. Figure 15 shows RMS value of lateral error (a) and angular error (b). As shown in the Figure 15, based on lateral error and angular error, we can say the controller has the best performance in three states: (1) in the dry road and velocities 30, 40m/s for all T values, (2) in the wet road and velocities 30, 40m/s for *T*s bigger and equal to 3s, (3) in frozen roads and velocity 30m/s for bigger and equal *T* values of 4s and for the velocity 40m/s for *T*s bigger and equal to 5s. The reason of unsuitable tracking in high velocities, low frictions, and small radius of curvatures is the saturation of lateral force on tires. In such a situation, the lateral tire force cannot resist against friction forces. In other words, a human driver would be also unable to appropriately control the vehicle. A possible solution to this issue is to use novel tires in which the adherence with the road is higher.

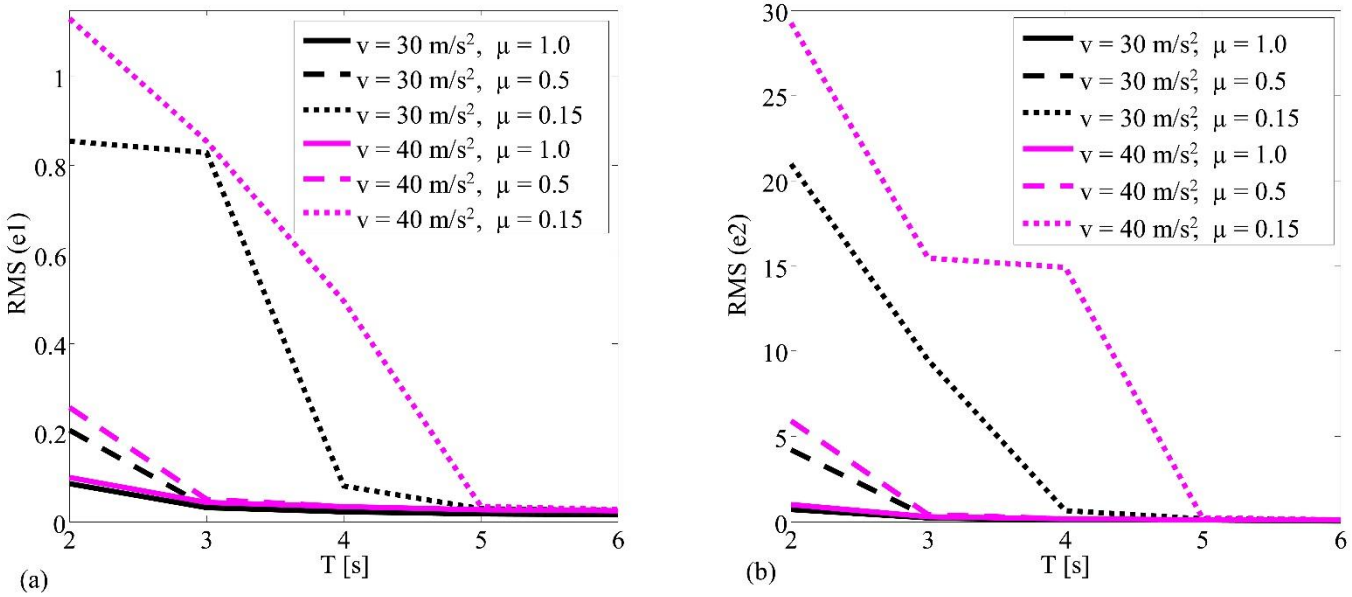

Figure 15 RMS value of lateral and angular error for different velocities, frictions and T values

Conclusion and further studies

In this paper, using the vehicle boundary conditions, the lane change path is designed for different maneuver times. For tracking the designed path, the adaptive sliding mode controller is designed. To avoid chattering and suitable control efforts, fuzzy boundary layer is applied. The designed controller in this study is simulated by linking the CarSim with

Simulink Software. This linkage provides a full vehicle model with higher DOF and taking the suspension, steering, non-linear tire subsystems, etc., into account. The simulation using this model is, to some extent, similar to real test environments. The simulation results show that the controller for dry road at different velocities and maneuver times has good performance. Also, in the wet road for different velocities and maneuver time equal or more than 3s, the controller showed good performance. In a frozen road, the controller for the velocity of 30m/s and maneuver time above 4s and for the velocity of 40m/s and maneuver time above 5s have good performance. In addition to high velocity, low friction, and short time lane change maneuver, non-linear behavior of tire models and the saturation of lateral forces on tires lead to unsuitable tracking. Thus, suitable duration of lane change maneuvers based on friction and longitudinal velocities has been presented. The designed controller can be tested in a real vehicle using a backstepping controller and in combination with sliding mode controller. It can be also optimized using a meta-heuristic algorithm. In addition, the study of Actuator/sensor faults in the vehicle dynamic model of 2-DOF by using of actuator faults via Markov chains[60, 62-64] deserve further investigation.

References

1. Wierwille W, Hanowski R, Hankey J, et al. Identification and evaluation of driver errors: overview and recommendations. US Department of Transportation, Federal Highway Administration. Report No. FHWA-RD-02-003, 2002.
2. Marshall JW. NHTSA Role in The Future of Automated Vehicles. *the 2013 AAMVA regional conference*. Dover, United Kingdom2013.
3. Chung T and Yi K. Design and evaluation of side slip angle-based vehicle stability control scheme on a virtual test track. *IEEE Transactions on control systems technology*. 2006; 14: 224-34.
4. Hiraoka T, Nishihara O and Kumamoto H. Automatic path-tracking controller of a four-wheel steering vehicle. *Vehicle System Dynamics*. 2009; 47: 1205-27.
5. Zhang J-m and Ren D-b. Lateral Control of Vehicle for Lane Keeping in Intelligent Transportation Systems. *Intelligent Human-Machine Systems and Cybernetics, 2009 IHMSC'09 International Conference on*. IEEE, 2009, p. 446-50.
6. Guo J, Li L, Li K and Wang R. An adaptive fuzzy-sliding lateral control strategy of automated vehicles based on vision navigation. *Vehicle System Dynamics*. 2013; 51: 1502-17.
7. Alipour H, Bannae Sharifian MB and Sabahi M. A modified integral sliding mode control to lateral stabilisation of 4-wheel independent drive electric vehicles. *Vehicle System Dynamics*. 2014; 52: 1584-606.
8. Li L, Wang H, Lian J, Ding X and Cao W. A lateral control method of intelligent vehicle based on fuzzy neural network. *Advances in Mechanical Engineering*. 2015; 7: 296209.
9. Hu C, Wang R and Yan F. Integral Sliding Mode-based Composite Nonlinear Feedback Control for Path Following of Four-Wheel Independently Actuated Autonomous Vehicles.
10. Lei J, Wu H, Yang J and Zhao J. Sliding mode lane keeping control based on separation of translation and rotation movement. *Optik-International Journal for Light and Electron Optics*. 2016; 127: 4369-74.
11. Soudbakhsh D and Eskandarian A. Comparison of linear and non-linear controllers for active steering of vehicles in evasive manoeuvres. *Proceedings of the institution of mechanical engineers, part I: Journal of Systems and Control Engineering*. 2012; 226: 215-32.
12. Zhang H and Wang J. Adaptive sliding-mode observer design for a selective catalytic reduction system of ground-vehicle diesel engines. *IEEE/ASME Transactions on Mechatronics*. 2016; 21: 2027-38.
13. Zhang H, Zhang G and Wang J. Sideslip Angle Estimation of an Electric Ground Vehicle via Finite-Frequency $\mathcal {H} _ {\infty} $ Approach. *IEEE Transactions on Transportation Electrification*. 2016; 2: 200-9.
14. Zhang H, Zhang G and Wang J. $\mathcal {H} _ {\infty} $ Observer Design for LPV Systems With Uncertain Measurements on Scheduling Variables: Application to an Electric Ground Vehicle. *IEEE/ASME Transactions on Mechatronics*. 2016; 21: 1659-70.
15. Yoshida H, Shinohara S and Nagai M. Lane change steering manoeuvre using model predictive control theory. *Vehicle System Dynamics*. 2008; 46: 669-81.
16. Attia R, Orjuela R and Basset M. Combined longitudinal and lateral control for automated vehicle guidance. *Vehicle System Dynamics*. 2014; 52: 261-79.
17. Choi M and Choi SB. MPC for vehicle lateral stability via differential braking and active front steering considering practical aspects. *Proceedings of the Institution of Mechanical Engineers, Part D: Journal of Automobile Engineering*. 2015: 0954407015586895.
18. Schildbach G and Borrelli F. Scenario model predictive control for lane change assistance on highways. *2015 IEEE Intelligent Vehicles Symposium (IV)*. IEEE, 2015, p. 611-6.
19. Brown M, Funke J, Erlien S and Gerdes JC. Safe driving envelopes for path tracking in autonomous vehicles. *Control Engineering Practice*. 2016.
20. Park J, Kim D, Yoon Y, Kim H and Yi K. Obstacle avoidance of autonomous vehicles based on model predictive control. *Proceedings of the Institution of Mechanical Engineers, Part D: Journal of Automobile Engineering*. 2009; 223: 1499-516.

21. Zhao C, Xiang W and Richardson P. Vehicle lateral control and yaw stability control through differential braking. *2006 IEEE International Symposium on Industrial Electronics*. IEEE, 2006, p. 384-9.
22. Li B and Yu F. Design of a vehicle lateral stability control system via a fuzzy logic control approach. *Proceedings of the Institution of Mechanical Engineers, Part D: Journal of Automobile Engineering*. 2010; 224: 313-26.
23. Song J. Integrated control of brake pressure and rear-wheel steering to improve lateral stability with fuzzy logic. *International Journal of Automotive Technology*. 2012; 13: 563-70.
24. Rastelli JP and Peñas MS. Fuzzy logic steering control of autonomous vehicles inside roundabouts. *Applied Soft Computing*. 2015; 35: 662-9.
25. Uzunsoy E and Erkilic V. Development of a trajectory following vehicle control model. *Advances in Mechanical Engineering*. 2016; 8: 1687814016650832.
26. Gong Y, Liu Y and Tang Z. Path tracking of unmanned vehicle based on parameters self-tuning fuzzy control. *Cyber Technology in Automation, Control and Intelligent Systems (CYBER), 2013 IEEE 3rd Annual International Conference on*. IEEE, 2013, p. 52-7.
27. Feng Y, Rongben W and Ronghui Z. Algorithm on lane changing and tracking control technology for intelligent vehicle. *Robotics and Biomimetics, 2007 ROBIO 2007 IEEE International Conference on*. IEEE, 2007, p. 1888-93.
28. Guo J, Hu P and Wang R. Nonlinear Coordinated Steering and Braking Control of Vision-Based Autonomous Vehicles in Emergency Obstacle Avoidance.
29. Suárez JI, Vinagre BM and Chen Y. A fractional adaptation scheme for lateral control of an AGV. *IFAC Proceedings Volumes*. 2010; 39: 149-54.
30. Petrov P and Nashashibi F. Adaptive steering control for autonomous lane change maneuver. *Intelligent Vehicles Symposium (IV), 2013 IEEE*. IEEE, 2013, p. 835-40.
31. Khosravi A, Lachini Z and Sarhadi P. Predictor-based model reference adaptive control for a vehicle lateral dynamics considering uncertainties. *Proceedings of the Institution of Mechanical Engineers, Part I: Journal of Systems and Control Engineering*. 2015; 229: 797-807.
32. Emirler MT, Wang H, Güvenç BA and Güvenç L. Automated Robust Path Following Control Based on Calculation of Lateral Deviation and Yaw Angle Error. *ASME 2015 Dynamic Systems and Control Conference*. American Society of Mechanical Engineers, 2015, p. V003T50A9-VT50A9.
33. Li H-m, Wang X-b, Song S-b and Li H. Vehicle Control Strategies Analysis Based on PID and Fuzzy Logic Control. *Procedia Engineering*. 2016; 137: 234-43.
34. Antonov S, Fehn A and Kugi A. A new flatness-based control of lateral vehicle dynamics. *Vehicle System Dynamics*. 2008; 46: 789-801.
35. Scalzi S, Benine-Neto A, Netto M, Pasillas-Lepine W and Mammar S. Active steering control based on piecewise affine regions. *Proceedings of the 2010 American Control Conference*. IEEE, 2010, p. 5362-7.
36. Anderson SJ, Peters SC, Pilutti TE and Iagnemma K. An optimal-control-based framework for trajectory planning, threat assessment, and semi-autonomous control of passenger vehicles in hazard avoidance scenarios. *International Journal of Vehicle Autonomous Systems*. 2010; 8: 190-216.
37. Mirzaei M, Alizadeh G, Eslamian M and Azadi S. An optimal approach to non-linear control of vehicle yaw dynamics. *Proceedings of the Institution of Mechanical Engineers, Part I: Journal of Systems and Control Engineering*. 2008; 222: 217-29.
38. Feng J, Ruan J and Li Y. Study on intelligent vehicle lane change path planning and control simulation. *2006 IEEE International Conference on Information Acquisition*. IEEE, 2006, p. 683-8.
39. Salehpour S, Pourasad Y and Taheri SH. Vehicle path tracking by integrated chassis control. *Journal of Central South University*. 2015; 22: 1378-88.
40. Enache NM, Mammar S, Lusetti B and Sebsadji Y. Active steering assistance for lane keeping and lane departure prevention. *Journal of Dynamic Systems, Measurement, and Control*. 2011; 133: 061003.
41. Li L, Lian J, Wang M and Li M. Fuzzy Sliding Mode Lateral Control of Intelligent Vehicle Based on Vision. *Advances in Mechanical Engineering*. 2013; 5: 216862.
42. Başlamişli SÇ, Köse İE and Anlaç G. Handling stability improvement through robust active front steering and active differential control. *Vehicle System Dynamics*. 2011; 49: 657-83.
43. Ji X, Wu J, Zhao Y, Liu Y and Zhao X. A new robust control method for active front steering considering the intention of the driver. *Proceedings of the Institution of Mechanical Engineers, Part D: Journal of Automobile Engineering*. 2015; 229: 518-31.
44. Jin XJ, Yin G and Chen N. Gain-scheduled robust control for lateral stability of four-wheel-independent-drive electric vehicles via linear parameter-varying technique. *Mechatronics*. 2015; 30: 286-96.
45. Saifizul A, Zainon M and Osman NA. An ANFIS Controller for Vision-based Lateral Vehicle Control System. *2006 9th International Conference on Control, Automation, Robotics and Vision*. IEEE, 2006, p. 1-4.
46. Sharma R, Kumar V, Gaur P and Mittal A. An adaptive PID like controller using mix locally recurrent neural network for robotic manipulator with variable payload. *ISA transactions*. 2016; 62: 258-67.
47. Zhang H and Wang J. Active steering actuator fault detection for an automatically-steered electric ground vehicle. *IEEE Transactions on Vehicular Technology*. 2017; 66: 3685-702.
48. Marino R, Scalzi S and Netto M. Integrated driver and active steering control for vision-based lane keeping. *European journal of control*. 2012; 18: 473-84.

49. Soudbakhsh D, Eskandarian A and Chichka D. Vehicle collision avoidance maneuvers with limited lateral acceleration using optimal trajectory control. *Journal of Dynamic Systems, Measurement, and Control*. 2013; 135: 041006.
50. Freeman P, Jensen M, Wagner J and Alexander K. A comparison of multiple control strategies for vehicle run-off-road and return. *IEEE Transactions on Vehicular Technology*. 2015; 64: 901-11.
51. Zhu X, Zhang H, Wang J and Fang Z. Robust Lateral Motion Control of Electric Ground Vehicles With Random Network-Induced Delays. *IEEE Transactions on Vehicular Technology*. 2015; 64: 4985-95.
52. Wang R, Jing H, Hu C, Chadli M and Yan F. Robust H∞ output-feedback yaw control for in-wheel motor driven electric vehicles with differential steering. *Neurocomputing*. 2016; 173: 676-84.
53. Jin X, Yin G, Bian C, Chen J, Li P and Chen N. Gain-Scheduled Vehicle Handling Stability Control Via Integration of Active Front Steering and Suspension Systems. *Journal of Dynamic Systems, Measurement, and Control*. 2016; 138: 014501.
54. Samiee S, Azadi S, Kazemi R and Eichberger A. Towards a Decision-Making Algorithm for Automatic Lane Change Manoeuvre Considering Traffic Dynamics. *PROMET-Traffic&Transportation*. 2016; 28: 91-103.
55. Rajamani R. *Vehicle dynamics and control*. Springer Science & Business Media, 2011.
56. Ackermann J. *Robust control: Systems with uncertain physical parameters*. Springer Science & Business Media, 2012.
57. He J, Crolla DA, Levesley M and Manning W. Coordination of active steering, driveline, and braking for integrated vehicle dynamics control. *Proceedings of the Institution of Mechanical Engineers, Part D: Journal of Automobile Engineering*. 2006; 220: 1401-20.
58. Slotine J-JE and Li W. *Applied nonlinear control*. prentice-Hall Englewood Cliffs, NJ, 1991.
59. Qiu J and Karimi HR. Fuzzy-Affine-Model-Based Memory Filter Design of Nonlinear Systems with Time-Varying Delay. *IEEE Transactions on Fuzzy Systems*. 2017.
60. Wei Y, Qiu J and Karimi HR. Reliable output feedback control of discrete-time fuzzy affine systems with actuator faults. *IEEE Transactions on Circuits and Systems I: Regular Papers*. 2017; 64: 170-81.
61. Barambones O, Garrido A, Maseda F and Alkorta P. An adaptive sliding mode control law for induction motors using field oriented control theory. *2006 IEEE Conference on Computer Aided Control System Design, 2006 IEEE International Conference on Control Applications, 2006 IEEE International Symposium on Intelligent Control*. IEEE, 2006, p. 1008-13.
62. Wei Y, Qiu J and Karimi HR. Quantized $\mathcal{H}\infty$ Filtering for Continuous-Time Markovian Jump Systems with Deficient Mode Information. *Asian Journal of Control*. 2015; 17: 1914-23.
63. Duan Z, Xiang Z and Karimi HR. Robust stabilisation of 2D state-delayed stochastic systems with randomly occurring uncertainties and nonlinearities. *International Journal of Systems Science*. 2014; 45: 1402-15.
64. Wei Y, Qiu J, Lam H-K and Wu L. Approaches to T–S fuzzy-affine-model-based reliable output feedback control for nonlinear Ito stochastic systems. *IEEE Transactions on fuzzy systems*. 2017; 25: 569-83.

Appendix I: The coefficients of vehicle equations based on error

$$a_{11} = -2\mu\frac{c_f + c_r}{mV_x} \qquad a_{21} = 2\mu\frac{l_r c_r - l_f c_f}{JV_x}$$
$$a_{12} = 2\mu\frac{c_f + c_r}{m} \qquad a_{22} = 2\mu\frac{l_f c_f - l_r c_r}{J}$$
$$a_{13} = 2\mu\frac{l_r c_r - l_f c_f}{mV_x} \qquad a_{23} = -2\mu\frac{c_f l_f^2 + c_r l_r^2}{JV_x}$$
$$b_1 = 2\mu\frac{c_f}{m} \qquad b_2 = 2\mu\frac{l_f c_f}{J}$$
$$d_1 = 2\mu\frac{l_r c_r - l_f c_f}{mV_x} - V_x \qquad d_2 = -2\mu\frac{c_f l_f^2 + c_r l_r^2}{JV_x}$$

Appendix II: Upper and lower bounds of uncertainties for controller design

$$\mathrm{a}_{\mathrm{ij}}^{+} = \mathrm{a}_{\mathrm{ij}}(\mu_2, \mathrm{v}_2) \qquad \mathrm{b}_{\mathrm{i}}^{+} = \mathrm{b}_{\mathrm{i}}(\mu_2, \mathrm{v}_2) \qquad \mathrm{d}_{\mathrm{i}}^{+} = \mathrm{d}_{\mathrm{i}}(\mu_2, \mathrm{v}_2) \qquad b = b_1 + db_2$$
$$\mathrm{a}_{\mathrm{ij}}^{-} = \mathrm{a}_{\mathrm{ij}}(\mu_1, \mathrm{v}_1) \qquad \mathrm{b}_{\mathrm{i}}^{-} = \mathrm{b}_{\mathrm{i}}(\mu_1, \mathrm{v}_1) \qquad \mathrm{d}_{\mathrm{i}}^{-} = \mathrm{d}_{\mathrm{i}}(\mu_1, \mathrm{v}_1) \qquad D = d_1 + dd_2$$
$$\hat{\mathrm{a}}_{\mathrm{ij}} = \frac{\mathrm{a}_{\mathrm{ij}}^{+} + \mathrm{a}_{\mathrm{ij}}^{-}}{2} \qquad \mathrm{b}^{-} = \mathrm{b}_1^{-} + \mathrm{db}_2^{-} \qquad D^{+} = \mathrm{d}_1^{+} + d\mathrm{d}_2^{+} \qquad \mathrm{A}_1 = \mathrm{a}_{11} + \mathrm{da}_{21}$$
$$\bar{\mathrm{a}}_{\mathrm{ij}} = \mathrm{a}_{\mathrm{ij}}^{+} - \hat{\mathrm{a}}_{\mathrm{ij}} \qquad \mathrm{b}^{+} = \mathrm{b}_1^{+} + d\mathrm{b}_2^{+} \qquad D^{-} = \mathrm{d}_1^{-} + d\mathrm{d}_2^{-} \qquad \mathrm{A}_2 = \mathrm{a}_{12} + \mathrm{da}_{22}$$
$$\hat{\mathrm{b}} = \sqrt{b^{+}b^{-}} \qquad \hat{\mathrm{D}} = \frac{D^{+} + D^{-}}{2} \qquad \mathrm{A}_3 = \mathrm{a}_{13} + \mathrm{da}_{23}$$
$$\bar{\mathrm{b}} = \mathrm{b}^{+} - \hat{\mathrm{b}} \qquad \bar{\mathrm{D}} = D^{+} - \hat{\mathrm{D}} \qquad \mathrm{A}_4 = \mathrm{A}_1 + \lambda$$
$$\mathrm{A}_5 = \mathrm{A}_3 + \lambda\mathrm{d}$$

$$f = \mathrm{A}_{11}\dot{\mathrm{e}}_1 + \mathrm{a}_{12}\mathrm{e}_2 + \mathrm{a}_{13}\dot{\mathrm{e}}_2 + \mathrm{b}_{12}\mathrm{u}_\mathrm{r} + \mathrm{d}_1\dot{\psi}_\mathrm{d}$$
$$f^{+} = \mathrm{A}_4^{+}\dot{\mathrm{e}}_1 + \mathrm{A}_2^{+}\mathrm{e}_2 + \mathrm{A}_5^{+}\dot{\mathrm{e}}_2 + D^{+}\dot{\psi}_\mathrm{d}$$

$$f^- = \mathrm{A}_4^-\dot{\mathrm{e}}_1 + \mathrm{A}_2^-\mathrm{e}_2 + \mathrm{A}_5^-\dot{\mathrm{e}}_2 + D^-\dot{\psi}_\mathrm{d}$$
$$\hat{\mathrm{f}} = \frac{f^+ + f^+}{2} = \widehat{\mathrm{A}}_4\dot{\mathrm{e}}_1 + \widehat{\mathrm{A}}_2\mathrm{e}_2 + \widehat{\mathrm{A}}_5\dot{\mathrm{e}}_2 + \widehat{\mathrm{D}}\dot{\psi}_\mathrm{d}$$
$$\left|f^+ - \hat{\mathrm{f}}\right| = \left|\overline{\mathrm{A}}_4\dot{\mathrm{e}}_1 + \overline{\mathrm{A}}_2\mathrm{e}_2 + \overline{\mathrm{A}}_5\dot{\mathrm{e}}_2 + \overline{\mathrm{D}}\dot{\psi}_\mathrm{d}\right| \leq \mathrm{F}$$
$$\mathrm{F} = \left|\overline{\mathrm{A}}_4\dot{\mathrm{e}}_1 + \overline{\mathrm{A}}_2\mathrm{e}_2 + \overline{\mathrm{A}}_5\dot{\mathrm{e}}_2 + \overline{\mathrm{D}}\dot{\psi}_\mathrm{d}\right|$$

Appendix II: The switching gain limit to evaluate Lyapunov stability

$$\gamma = \sqrt{\frac{\mathrm{b}^+}{\mathrm{b}^-}} = \sqrt{\frac{\mu_2}{\mu_1}}$$
$$\mathrm{b}^- \leq b \leq \mathrm{b}^+$$
$$\sqrt{\frac{\mathrm{b}_{11}^-}{\mathrm{b}_{11}^+}} \leq \mathrm{b}\hat{\mathrm{b}}^{-1} \leq \sqrt{\frac{\mathrm{b}_{11}^+}{\mathrm{b}_{11}^-}}$$
$$\gamma^{-1} \leq \mathrm{b}\hat{\mathrm{b}}^{-1} \leq \gamma$$
$$-\gamma^{-1} \geq -\mathrm{b}\hat{\mathrm{b}}^{-1} \geq -\gamma$$
$$\left|1 - \mathrm{b}\hat{\mathrm{b}}^{-1}\right| \leq |1-\gamma^{-1}|$$
$$-\gamma^{-1} \geq -\mathrm{b}\hat{\mathrm{b}}^{-1}$$